

Article

DFT Study on the Interaction of the Smallest Fullerene C₂₀ with Lithium Ions and Atoms

Hiroshi Kawabata * and Hiroto Tachikawa

Division of Applied Chemistry, Graduate School of Engineering, Hokkaido University, Sapporo 060-8628, Japan; hiroto@eng.hokudai.ac.jp

* Correspondence: kawabata1041@nifty.com

Academic Editor: Tomoya Takada

Received: 28 March 2017; Accepted: 28 April 2017; Published: 10 May 2017

Abstract: The smallest fullerene C₂₀ with positive electron affinity is considered to be a new organic nano-electronic material. The binding structures and electronic states of lithium ions and atoms (Li⁺ and Li) trapped on the surface of C₂₀ have been investigated by means of density functional theory (DFT) calculation to elucidate the nature of their interaction. It was found that a Li⁺ can bind to only one site of C₂₀. This is, specifically, on top of the site where Li⁺ binds to the carbon atom of C₂₀. On the other hand, in the case of a Li atom, two structures were obtained besides the on-top structure. One was pentagonal structure which included a Li atom on a five-membered ring of C₂₀. The other was a triangular structure in which the Li atom bind to the the carbon–carbon bond of C₂₀. Finally, the nature of the interactions between Li ions or atoms and the C₂₀ cluster was discussed on the basis of theoretical results.

Keywords: C₂₀ fullerene; alkali metal; organic electronic materials; binding energy; transition state; diffusion mechanism; density functional theory

1. Introduction

Currently, the diameter of the thinnest carbon nanotube synthesized is 4 Å, and its tip is expected to have a structure similar to that of a C₂₀ fullerene [1]. It has been reported by photoelectron spectroscopy that C₂₀ is predicted to be the smallest fullerene that is synthesized from vapor growth, and that its electron affinity is positive [2,3]. Its structure is very simple and highly symmetrical, consisting of 12 five-membered rings only. Its diameter is about 4 Å, which is less than half of that of C₆₀ fullerene. It is also known to form one-dimensional chains, the key to a controlled structure, via vapor deposition using an arc plasma gun [4]. C₂₀ and its derivatives are considered to be not only new n-type materials, but also ultimate organic nanomaterials capable of controlling size and orientation.

In order to utilize this organic molecule as an electronic material, knowledge of fundamental physical properties as to how its electronic state is changed by doping is very important. The interaction of C₆₀ with alkali metal is investigated by various methods such as spectroscopy and electrochemical methods [5–10]. In particular, superconductivity is reported to occur in systems doped with K atoms [10]. It is also well known that alkali metal-doped nanostructures are promising for technical applications such as gas storage and the mobilization of small organic molecules [11,12]. For these reasons, it is important to know the exact structure and electronic properties of the systems interacting with alkali metals. We are particularly interested in chemical stability, reactivity of C₂₀, and the change of electronic state by doping. However, basic data on the doping state of C₂₀ is rarely found in experimental research as well as in theoretical research.

Recently, we studied the structures and electronic states of alkyl and hydroxyl radical functionalized C₂₀ fullerene [13,14]. We also studied the binding structures and electronic states

of sodium ions and atoms trapped on the surface of C_{20} [15]. However, the interaction between C_{20} and Li^+ ions or Li atoms, as well as its reaction mechanisms have never been studied so far.

Tachikawa theoretically investigated the diffusion dynamics of an Li^+ ion on the surface of C_{60} fullerene by the direct dynamics method [16,17]. This study revealed two transition states (TSs) of Li^+ ion diffusion. It also revealed that a Li^+ ion diffuses along the node faces of the highest occupied molecular orbital (HOMO) of C_{60} and graphene [17,18]. However, the interaction between C_{20} and other alkali metals, the transition states of the reaction, and the migration path on the surface have not yet been elucidated.

In this study, the interactions of Li^+ ions and Li atoms with C_{20} were investigated by means of density functional theory (DFT) to clarify their binding site and TS.

2. Results and Discussion

2.1. C_{20} - Li^+

2.1.1. Optimized Structure of the C_{20} - Li^+ System

The structures of C_{20} and C_{20} - Li^+ were fully optimized at the CAM-B3LYP level. The structure obtained is illustrated Figure 1. The only stable structure of C_{20} - Li^+ was the on-top structure with a Li^+ ion on C0. In the pentagonal structure where a Li^+ ion is on the carbon five-membered ring, there was a vibration mode of the imaginary part. Thus, it was not a stationary point in this system. The distance $R1$ between C0 and Li of the on-top structure was 2.055 Å, and the angle $\theta1$ of $\angle C1-C0-Li$ was 121 degrees (Table 1). The $Li-C0$ stretching mode (ν_{C0-Li^+}) was calculated to be 399 cm^{-1} . In our previous research, the hexagonal structure and pentagonal structure were more stable than the on-top structure in C_{60} - Li^+ [16]. In addition, it is known that the Li^+ ion on graphene has a hexagonal structure. The on-top structure is a structure unique to C_{20} - Li^+ , which seems to be related to the curvature of C_{20} .

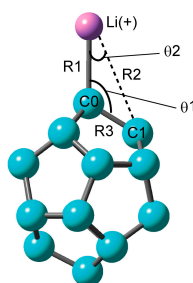


Figure 1. Optimized structure of C_{20} - Li^+ calculated at the CAM-B3LYP/6-311+G(d) level.

Table 1. Optimized structural parameters, natural population analysis (NPA) atomic charge on C0 and Li^+ , and binding energies of Li^+ to C_{20} calculated at several levels of theory. Zero point energy corrected values are in parentheses.

Method	Structural Parameter					NPA Atomic Charge		$E_{bind}^{(a)}/kcal\ mol^{-1}$
	$R1/\text{Å}$	$R2/\text{Å}$	$\theta1/^\circ$	$\theta2/^\circ$	ν_{C0-Li^+}/cm^{-1}	C0	Li^+	
CAM-B3LYP/6-311G(d)	2.0548	3.1288	121.0	24.7	399	-0.630	0.957	43.24 (41.31)
CAM-B3LYP/6-311+G(d)	2.0547	3.1293	121.0	24.7	399	-0.621	0.955	42.36 (40.40)

^(a) The energy of the Li^+ ion binding to C_{20} (E_{bind}) is defined by $-E_{bind} = E(C_{20}-Li^+) - [E(C_{20}) + E(Li^+)]$. Here, $E(C_{20}-Li^+)$ represents the total energy of the Li^+ ion added to C_{20} , $E(C_{20})$ represents that of the free C_{20} molecule, and $E(Li^+)$ represents that of the free Li^+ ion, respectively.

The natural population analysis (NPA) atomic charges on the Li^+ ion and C0 were +0.955 and -0.621, respectively. These results imply that the Li^+ ion and C0 atom have a positive and

a negative charge, respectively. The C0–Li bond is polarized. The binding energy was calculated to be $42 \text{ kcal}\cdot\text{mol}^{-1}$. This energy is significantly larger than the binding energy for the $\text{C}_{60}\text{--Li}^+$ system [16]. The binding energy of the on-top structure of $\text{C}_{60}\text{--Li}^+$ was about $30 \text{ kcal}\cdot\text{mol}^{-1}$, and it was found that $\text{C}_{20}\text{--Li}^+$ produces a stronger bond than $\text{C}_{60}\text{--Li}^+$.

2.1.2. Electronic Structures of Pure C_{20} and $\text{C}_{20}\text{--Li}^+$

Figure 2 shows the highest occupied molecular orbital (HOMO) and the lowest unoccupied molecular orbital (LUMO) of C_{20} and $\text{C}_{20}\text{--Li}^+$. When doping with Li^+ ions, the electronic state of C_{20} changes drastically. The molecular orbital is spread between C0 and Li^+ at HOMO. The energy difference between the HOMO and LUMO orbitals of C_{20} is 4.2 eV, that is, C_{20} acts as an insulator. Using the optimized structure of C_{20} and $\text{C}_{20}\text{--Li}^+$, the vertical excitation energies were calculated by TD-CAMB3LYP/6-311+G(d). The first excitation energies (S_1) of C_{20} and $\text{C}_{20}\text{--Li}^+$ were 3.01 eV and 1.48 eV, respectively. These results mean that a charge transfer occurs between C_{20} and Li^+ at HOMO.

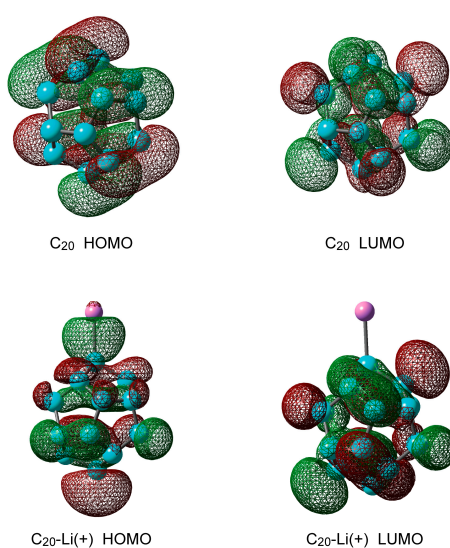


Figure 2. Molecular orbitals of C_{20} and $\text{C}_{20}\text{--Li}^+$ calculated at the CAM-B3LYP/6-311+G(d) level.

The electronic states of C_{20} will be changed by the doping of the Li^+ ion. To elucidate the electronic states of the binding site, natural bond orbital (NBO) analysis was carried out for the $\text{C}_{20}\text{--Li}^+$ system. The NBO of the C0–C1 bond of pure C_{20} was expressed by:

$$\sigma_{\text{C0-C1}} = 0.701 (\text{sp}^{2.03})_{\text{C0}} + 0.713 (\text{sp}^{2.03})_{\text{C1}}$$

where, C0 and C1 indicate the carbon atom in the addition center and the neighbor-positioned carbon atom, respectively.

After the Li^+ ion doping to C_{20} , the NBO was changed to be:

$$\sigma_{\text{C0-C1}} = 0.690 (\text{sp}^{2.72})_{\text{C0}} + 0.724 (\text{sp}^{2.05})_{\text{C1}}$$

Before the doping of Li^+ ion, the carbon atom in the doping site (C0) takes an electronic state of $\text{sp}^{2.03}$. After the doping, the state was changed to $\text{sp}^{2.72}$. This result indicates that the carbon atom (C0) is changed from sp^2 to sp^3 .

2.1.3. Transition State of $\text{C}_{20}\text{--Li}^+$ and the Movement Path of the Li Ion on the Surface of C_{20}

Figure 3 shows the structure of the transition state of $\text{C}_{20}\text{--Li}^+$ and its energy diagram. The structure of the transition state was found to be a triangular structure with the Li^+ ion on the C–C bond (Table 2).

Intrinsic reaction coordinate (IRC) analysis was performed, and it was confirmed that the Li^+ ion migrated from C0 (RC, reactant) onto the adjacent carbon (C1) (PD, product) via the triangular structure as the transition state. Its activation energy (E_{act}) is as high as about $12 \text{ kcal}\cdot\text{mol}^{-1}$. The structure of the transition state in which the Li^+ ion diffuses onto C_{60} is also a triangular structure. However, its activation energy is less than $4 \text{ kcal}\cdot\text{mol}^{-1}$. In other words, the movement of the Li^+ ion on the surface of C_{20} is like a bond alternation. It cannot be said that the Li^+ ion diffuses by heat.

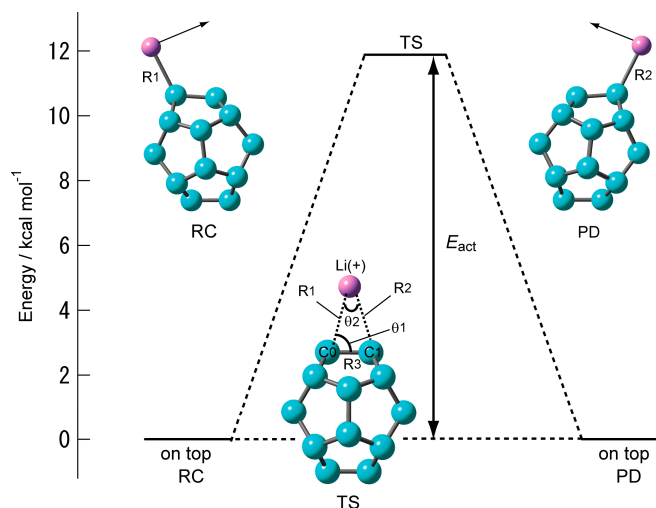


Figure 3. Energy diagram of Li^+ ion migration reaction on the surface of C_{20} calculated at the CAM-B3LYP/6-311+G(d) level.

Table 2. Structural parameters of the transition state and activation energies (E_{act} in $\text{kcal}\cdot\text{mol}^{-1}$) calculated at several levels of theory. Zero point energy corrected values are in parentheses.

System	Structural Parameter					$E_{\text{act}}/\text{kcal}\cdot\text{mol}^{-1}$
	R1/Å	R3/Å	$\theta 1/^{\circ}$	$\theta 2/^{\circ}$	$\nu_{\text{C0-Li}^+}/\text{cm}^{-1}$	
CAM-B3LYP/6-311G(d)	2.2856	1.4347	71.7	36.6	399 <i>i</i>	11.94 (11.34)
CAM-B3LYP/6-311+G(d)	2.2884	1.4352	71.7	36.5	400 <i>i</i>	11.88 (11.31)

2.2. $\text{C}_{20}\text{-Li}$

2.2.1. Optimized Structure of $\text{C}_{20}\text{-Li}$

The structures of $\text{C}_{20}\text{-Li}$ optimized at the CAM-B3LYP/6-311+G(d) level are illustrated in Figure 4. Three structures were found in $\text{C}_{20}\text{-Li}$, an on-top structure where the Li atom is located on the carbon atom, a triangular structure where the Li atom binds to the center of the C–C bond (triangle), and a pentagonal structure where the Li atom is located in the center of the five-membered ring (pentagon). There was no vibration mode of the imaginary part. That is, the structures are stationary points, respectively. Very interestingly, the triangular structure, which was in the transition state of $\text{C}_{20}\text{-Li}^+$, was the most stable in $\text{C}_{20}\text{-Li}$. This means that the movement path of the Li^+ ion and Li atom on the surface of C_{20} can be controlled by an electric charge.

The C0–Li distance of $\text{C}_{20}\text{-Li}$ of the on-top structure is about 0.1 \AA shorter than that of $\text{C}_{20}\text{-Li}^+$. In the triangular structure, the C0–Li distance is about 0.3 \AA shorter than that of $\text{C}_{20}\text{-Li}^+$. In other words, $\text{C}_{20}\text{-Li}$ formed in the on-top structure and triangular structure is thought to have larger binding energy and charge transfer than $\text{C}_{20}\text{-Li}^+$.

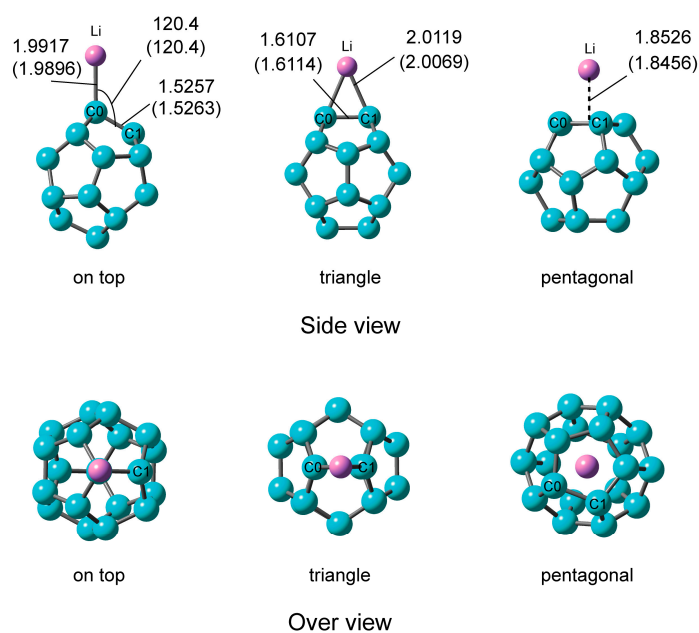


Figure 4. Optimized structures of C_{20} -Li system; on top, triangular, and pentagonal structures calculated at the CAM-B3LYP/6-311+G(d). In parentheses, values were calculated at the CAM-B3LYP/6-311G(d) level. The bond distances and angles are in Å and in degrees, respectively.

The binding energy and NPA atomic charge of each atom of C_{20} -Li calculated at the CAM-B3LYP/6-311+G(d) level are provided in Table 3. The NPA atomic charge of the Li atom in the on-top, the triangular, and the pentagonal sites were +0.934, +0.869, and +0.823, respectively.

Table 3. Binding energies of Li to C_{20} , and NPA atomic charges of C_{20} , C0, and Li calculated at the CAM-B3LYP/6-311+G(d) level. Zero point energy corrected values are in parentheses.

System	$E_{\text{bind}}^{(b)}/\text{kcal}\cdot\text{mol}^{-1}$	NPA Atomic Charge		
		Part of C_{20}	C(0)	Li
On-top	49.42 (49.32)	-0.934	-0.662	+0.934
Triangle	52.96 (52.85)	-0.869		+0.869
Pentagonal	46.89 (47.95)	-0.823		+0.823

^(b) The energy of the Li atom binding to C_{20} (E_{bind}) is defined by $-E_{\text{bind}} = E(C_{20}\text{-Li}) - [E(C_{20}) + E(\text{Li})]$. Here, $E(C_{20}\text{-Li})$ represents the total energy of the Li atom added to C_{20} , $E(C_{20})$ represents that of the free C_{20} molecule, and $E(\text{Li})$ represents that of the free Li atom, respectively.

In all structures, it can be seen that the charge of C_{20} is changed to negative due to the addition of the Li atom, indicating that charge transfer occurs from Li to C_{20} . The magnitude of the dipole moment is 11.3 D, 7.2 D, and 6.7 D in each of the on-top, triangular, and pentagonal structures, which is related to the charge transfer amount.

The binding energy between C_{20} and the Li atom was 49.42 kcal mol⁻¹ for on-top structure, 52.96 kcal mol⁻¹ for triangular structure, and 46.89 kcal mol⁻¹ for pentagonal structure. These binding energies are 4.5–10.6 kcal mol⁻¹ greater than that of C_{20} -Li⁺. This is due to the fact C_{20} -Li produces a strong charge transfer to C_{20} rather than C_{20} -Li⁺.

The electronic states of C_{20} were changed by the doping of Li atoms as well as that of C_{20} -Li⁺. To elucidate the electronic states of the interaction site, natural bond orbital (NBO) analysis was carried out for the C_{20} -Li system. The NBO of the C0-C1 bond of C_{20} -Li was expressed by:

$$\sigma_{\text{C0-C1}} (\text{on top}) = 0.695 (sp^{2.72})_{\text{C0}} + 0.719 (sp^{2.06})_{\text{C1}}$$

$$\sigma_{C0-C1} \text{ (triangle)} = 0.707 (sp^{3.13})_{C0} + 0.707 (sp^{3.13})_{C1}$$

$$\sigma_{C0-C1} \text{ (pentagonal)} = 0.707 (sp^{2.14})_{C0} + 0.708 (sp^{2.15})_{C1}$$

where, C0 and C1 are carbon atoms of C₂₀ (see Figure 4). After the doping, the electronic states of the on-top and triangular structures were drastically changed. These results indicate that the electronic state in the carbon atom (C0) is changed from sp² to sp³. In contrast, the hybridization of C0 was hardly changed in the pentagonal structure. It seems that, in this case, the interaction of the Li–C bond was spread into five carbon atoms.

2.2.2. Transition State of C₂₀–Li and the Movement Path of the Li atom on the Surface of C₂₀

Figure 5 shows the structures of the transition state and energy diagram of C₂₀–Li. When the position of the Li atom changes from the on-top site and pentagonal site to the triangular site, it turns out that there is one transition state in each. The transition state when changing from the on-top structure to the triangular structure is TS-1, and the transition state when changing from the pentagonal structure to the triangular structure is TS-2. TS-1 and TS-2 each has a vibrational mode of one imaginary part. IRC confirmed that the on-top structure and the pentagonal structure are triangular structures via TS-1 and TS-2, respectively.

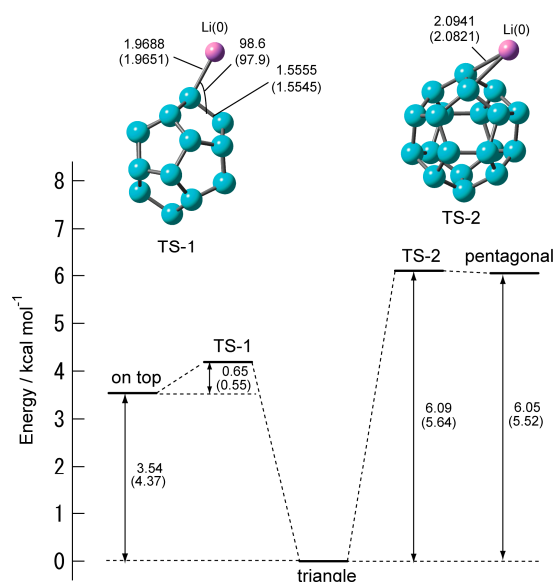


Figure 5. Energy diagram and structures of the transition state of C₂₀–Li system calculated at the CAM-B3LYP/6-311+G(d) level. In parentheses are the values calculated at the CAM-B3LYP/6-311G(d) level.

Table 4 shows the activation energies (E_{act}) and the vibrational frequencies for the imaginary modes. TS-1 and TS-2 have one vibration mode of the imaginary part, respectively. Both E_{act} of TS-1 and TS-2 were less than 1 kcal·mol⁻¹. This was significantly smaller than that of the E_{act} of the C₂₀–Li⁺. This means that the on-top structure and the pentagonal structures are easily changed to the triangular structure by thermal activation. However, the triangular structure is 6.1 kcal mol⁻¹ more stable than the pentagonal structure. Therefore, it is unlikely that the Li atom will diffuse the surface of C₂₀ via TS-2.

Table 4. The activation energies (E_{act} in kcal mol⁻¹) and imaginary frequencies (ν_i in cm⁻¹) of TS-1 and TS-2 in the C₂₀-Li system calculated at the CAM-B3LYP/6-311+G(d) level. In parentheses, values were calculated at the CAM-B3LYP/6-311G(d) level.

State	$E_{\text{act}}/\text{kcal mol}^{-1}$	ν_i/cm^{-1}
TS-1	0.65 (0.55)	252 <i>i</i> (182 <i>i</i>)
TS-2	0.04 (0.12)	110 <i>i</i> (120 <i>i</i>)

On the other hand, the difference in heat of formation between the triangular structure and the on-top structure is 3.5 kcal mol⁻¹. The activation energy for Li⁺ ions to diffuse onto the surface of C₆₀ is ca. 4 kcal mol⁻¹ [16]. Thus, there is a possibility that the Li atom diffuses its surface along the C-C bond of C₂₀.

3. Method of Calculation

All hybrid DFT calculations were carried out using the Gaussian 09 program package [19]. Clusters of C₂₀ and Li⁺ ions or Li atoms were examined. All calculations performed in this study are only Γ points. The structures and electronic states of C₂₀, C₂₀-Li⁺ (denoted by C₂₀-Li⁺), and C₂₀-Li atom (denoted by C₂₀-Li) were calculated using the CAM-B3LYP functional, which produces accurate results for long-range interactions, and these results were combined with several basis sets [20–23]. Calculations on C₂₀ and C₂₀-Li⁺ were performed using the RCAM-B3LYP functional. Since C₂₀-Li is an open shell, the calculation was made using the UCAM-B3LYP functional. The geometries of all systems were fully optimized at the CAM-B3LYP/6-311G(d) and CAM-B3LYP/6-311+G(d) levels of theory. The convergence criterion of SCF (self-consistent field) was set to 10⁻⁷. These levels of theory have given reasonable electronic structures of C₂₀-Li⁺ and C₂₀-Li systems [13–15,24,25]. All of the geometries studied here were characterized as stationary or transition states by analytically vibrational frequency calculation.

Furthermore, each transition state was checked to be connected to the initial state and the final state by IRC analysis.

4. Conclusions

In this study, the interaction between C₂₀ and Li⁺ ions and Li atoms were investigated by density functional theory. The only stable structure of C₂₀-Li⁺ is the on-top structure, where the Li⁺ ion is on top of the carbon atom of C₂₀. The Li⁺ ion migrates to an adjacent carbon atom through a triangular structure consisting of C-C and Li⁺. Its activation energy is 12 kcal·mol⁻¹, and the migration of the Li⁺ ion is due to coupling substitution. On the other hand, C₂₀-Li has three structures: the on-top structure, triangular structure, and pentagonal structure. The most stable is the triangular structure, while the other two are metastable. The activation energy from on-top structure and pentagonal structure to the triangular structure is smaller than 1 kcal·mol⁻¹. From the magnitude of the relative energy of each structure, it was revealed that the Li atom diffuses with heat along the C-C bond of C₂₀.

Acknowledgments: The author acknowledges partial support from JSPS KAKENHI Grant Number 15K05371 and MEXT KAKENHI Grant Number 25108004.

Author Contributions: Hiroshi Kawabata and Hiroto Tachikawa designed this study and wrote the paper; All of the computer experiments and analyses were conducted by Hiroshi Kawabata.

Conflicts of Interest: The authors declare no conflict of interest.

References

1. Qin, L.-C.; Zhao, X.; Hirahara, K.; Miyamoto, Y.; Ando, Y.; Iijima, S. The smallest carbon nanotube. *Nature* **2000**, *408*, 50. [[CrossRef](#)] [[PubMed](#)]
2. Parasuk, V.; Almof, J. C₂₀: The smallest fullerene? *Chem. Phys. Lett.* **1991**, *184*, 187–190. [[CrossRef](#)]

3. Prinzbach, H.; Weiler, A.; Landenberger, P.; Wahl, F.; Wörth, J.; Scott, L.T.; Gelmont, M.; Olevano, D.; Issendorff, B.V. Gas-phase production and photoelectron spectroscopy of the smallest fullerene, C₂₀. *Nature* **2000**, *407*, 60–63. [[CrossRef](#)] [[PubMed](#)]
4. Kurokawa, S.; Yamamoto, D.; Hirashige, K.; Sakai, A. Possible formation of one-dimensional chains of C₂₀ fullerenes observed by scanning tunneling microscopy. *Appl. Phys. Express* **2016**, *9*, 045102. [[CrossRef](#)]
5. Lüsse, B.; Riede, M.; Leo, K. Doping of organic semiconductor. *Phys. Status. Solidi. A* **2013**, *210*, 9–43.
6. Salzmann, I.; Heimel, G. Toward a comprehensive understanding of molecular doping organic semiconductors. *J. Electron Spectrosc. Relat. Phenom.* **2015**, *204*, 208–222. [[CrossRef](#)]
7. Holczer, K.; Whetten, R.L. Superconducting and normal state properties of the A₃C₆₀ compounds. *Carbon* **1992**, *30*, 1261–1276. [[CrossRef](#)]
8. Moriyama, H.; Kobayashi, H.; Kobayashi, A.; Watanabe, T. ESR spectra on single crystals of alkali metal fulleride complexes by means of wet-chemical synthesis. *Chem. Phys. Lett.* **1995**, *238*, 116–121. [[CrossRef](#)]
9. Dalchiele, E.A. Rosolen. J.M.; Decker, F. Electrochemically intercalated M_xC₆₀ thin films in a solid state cell (M = Li, K): Optical and photoelectrochemical characterization. *Appl. Phys. A Mater. Sci.* **1996**, *63*, 487–494.
10. Zhang, Z.; Chen, C.C.; Kelty, S.P.; Dai, H.J.; Lieber, C.M. The superconducting energy gap of Rb₃C₆₀. *Nature* **1991**, *353*, 333–335. [[CrossRef](#)]
11. Cazorla, C.; Shevlin, S.A.; Guo, Z.X. Calcium-based functionalization of carbon materials for CO₂ capture: A first-principles computational study. *J. Phys. Chem. C* **2011**, *115*, 10990–10995. [[CrossRef](#)]
12. Cazorla, C. Ab initio study of the binding of collagen amino acids to graphene and A-doped (A = H, Ca) graphene Original Research Article. *Thin Solid Films* **2010**, *518*, 6951–6961. [[CrossRef](#)]
13. Abe, S.; Kawano, S.; Toida, Y.; Nakamura, M.; Inoue, S.; Sano, H.; Yoshida, Y.; Kawabata, H.; Tachikawa, H. Electronic states of alkyl-radical-functionalized C₂₀ fullerene using density functional theory. *Jpn. J. Appl. Phys.* **2016**, *55*, 03DD03. [[CrossRef](#)]
14. Iyama, T.; Abe, S.; Tachikawa, H. Density functional theory (DFT) study on the addition of hydroxyl radical (OH) to C₂₀. *Mol. Cryst. Liq. Cryst.* **2012**, *567*, 200–206. [[CrossRef](#)]
15. Fukuzumi, T.; Tachikawa, H.; Azumi, K. DFT Study on the interaction of carbon nano-materials with sodium ion and atom. *Mol. Cryst. Liq. Cryst.* **2011**, *538*, 61–66. [[CrossRef](#)]
16. Tachikawa, H. Diffusion of the Li⁺ Ion on C₆₀: A DFT and Molecular Dynamics Study. *J. Phys. Chem. C* **2011**, *115*, 20406–20411. [[CrossRef](#)]
17. Tachikawa, H. Diffusion dynamics of the Li ion on C₆₀: A direct molecular orbital–molecular dynamics study. *J. Phys. Chem. C* **2007**, *111*, 13087–13091. [[CrossRef](#)]
18. Tachikawa, H.; Shimizu, A. Diffusion Dynamics of the Li⁺ Ion on a Model Surface of Amorphous Carbon: A direct molecular orbital dynamics study. *J. Phys. Chem. B* **2005**, *109*, 13255–13262. [[CrossRef](#)] [[PubMed](#)]
19. *Gaussian 09, Revision D.01*, Gaussian, Inc.: Wallingford CT, 2013.
20. Kobayashi, R.; Amos, R.D. The application of CAM-B3LYP to the charge-transfer band problem of the zincbacteriochlorin–bacteriochlorin complex. *Chem. Phys. Lett.* **2006**, *420*, 106–109. [[CrossRef](#)]
21. Yanai, T.; Tew, D.P.; Handy, N.C. A new hybrid exchange–Correlation functional using the Coulomb-attenuating method (CAM-B3LYP). *Chem. Phys. Lett.* **2004**, *393*, 51–57. [[CrossRef](#)]
22. Cazorla, C.; Shevlin, S.A. Accuracy of density functional theory in the prediction of carbon dioxide adsorbent materials. *Dalton Trans.* **2013**, *42*, 4670–4676. [[CrossRef](#)] [[PubMed](#)]
23. Cazorla, C. The role of density functional theory methods in the prediction of nanostructured gas-adsorbent materials. *Coordination Chem. Rev.* **2015**, *300*, 142–163. [[CrossRef](#)]
24. Tachikawa, H.; Kawabata, H. Electronic states of alkali metal-NTCDA complexes: A DFT study. *Solid State Sci.* **2015**, *48*, 141–146. [[CrossRef](#)]
25. Iyama, T.; Kawabata, H.; Tachikawa, H. Origin of Spectrum Shifts of Benzophenone-Water Clusters: DFT Study. *J. Solution Chem.* **2014**, *43*, 1676–1686. [[CrossRef](#)]

